RSC Advances

PAPER

View Article Online
View Journal | View Issue

Cite this: *RSC Adv.*, 2018, **8**, 35850

Rapid and visual readout of vitamin B1 based on the electrostatic interaction induced aggregation of gold nanoparticles†

Liping Lin,*[a] Jiajing Wang,[a] Wei Liu,[b] Yaxin Luo,[a] Yanling Xiao[a] and Yuhan Wang[a]

Received 1st October 2018
Accepted 11th October 2018

DOI: 10.1039/c8ra08153k

rsc.li/rsc-advances

In this work, a simple and rapid colorimetric assay for the quantitative detection of vitamin B1 (VB1) has been fabricated based on citrate-stabilized gold nanoparticles (AuNPs). The UV-Vis spectra of AuNPs varied and the relative color changed from red to purple with the sequential addition of VB1. The characterization results of AuNPs with and without the addition of VB1 confirmed that the observed phenomena were attributed to the aggregation of AuNPs induced by VB1 through electrostatic interaction. The assay was rapid and sensitive to VB1 with a detection limit of 10.9 nM ranging from 30 nM to 650 nM in 15 min. Meanwhile, the developed assay displayed excellent selectivity to VB1 since AuNPs showed negligible response to common metal ions and biological molecules. Moreover, the feasibility for the quantitative detection of VB1 in tablets and human urine samples has also been demonstrated.

Introduction

Vitamin B1 (VB1), also named as thiamine, contains an aminopyrimidine ring and a thiazole ring with methyl and hydroxyethyl side chains linked by a methylene bridge. As is known, VB1 is an essential water-soluble vitamin and natural nutrient present in our dairy foods[1] with the average daily intake of 0.5–1 mg.[2] It plays a crucial role in the metabolic processes of carbohydrate, amino acids and lipids in living systems.[3,4] Additionally, as a biologically and pharmaceutically important compound, VB1 is necessary to maintain the proper functioning of the heart, nerves and cardiovascular system.[5] VB1 deficiency causes numerous deleterious effects on human beings. Most notably, VB1 deficiency is responsible for beriberi (a chronic neurological and cardiovascular disease)[6] and Wernicke–Korsakoff syndrome (caused brain abnormalities)[7] due to malnutrition and chronic alcoholism. Moreover, the abnormal level of VB1 has also been implicated in Alzheimer's disease.[8] Results from Ke's work indicated that VB1 malnutrition was associated with depression among older Chinese adults.[9] Therefore, it is highly crucial to explore a simple, fast and accurate method to detect and monitor the levels of VB1 in these patients to promote a quick recovery.

Up to now, various methods have been employed to assay VB1, such as high performance liquid chromatography (HPLC),[10] chemiluminescence (CL) method,[11] absorption spectrometric assay,[12,13] potentiometric assay,[14] fluorimetry,[15–20] resonance Rayleigh scattering spectral method[21] and so on. Among these analytical techniques, the problems like inevitable use of organic solvents in HPLC and CL, poor reproducibility of potentiometric assay, expensive instruments for resonance Rayleigh scattering spectral method, special competitive reaction between VB1 and fluorescent materials with the metal ions in some extent limited their wide applications. Absorption spectrometric assay, by contrast, has aroused much attention due to its excellent attributes including simple and rapid operations without any complicated instruments, high reproducibility and low-cost and some even can be observed with the naked eye. Therefore, colorimetric assays with the aid of ultraviolet absorption spectra have aroused much attention from the researchers.

Gold nanoparticles (AuNPs) endow a tremendous extinction coefficient with several orders of magnitude greater than those for traditional organic chromophores,[22] which promises the high sensitivity for AuNPs based methods. Moreover, the localized surface plasmon resonance (LSPR) of AuNPs has close relationship with their size, shape, composition, interparticle distance and the dielectric constant of their surrounding medium.[23] And the shorten interparticle distance will cause a redshift in the LSPR band(s) with an increase in intensity and an observable visualization of color change from burgundy for individual AuNPs to blue for aggregated ones. Meanwhile, colorimetric assays exhibit excellent analytical performances in terms of simple operation, fast response and convenience without any expensive or complex instrumentation. Taking in

[a]*Department of Applied Chemistry, College of Life Sciences, Fujian Agriculture and Forestry University, Fuzhou, 350002, China. E-mail: linliping2015@fafu.edu.cn; Tel: +86 18859279026*

[b]*Department of Bioinformatics, College of Life Sciences, Fujian Agriculture and Forestry University, Fuzhou, 350002, China*

† Electronic supplementary information (ESI) available. See DOI: 10.1039/c8ra08153k

the above objectives into consideration, colorimetric assays based on the mechanism that analytes induce dispersed AuNPs to aggregated ones have been proposed for the *situ* monitor of many different analytes in environmental and biological fields.[11,24–28]

Herein, we proposed a rapid, simple, highly sensitive and selective assay for the colorimetric detection of VB1 with citrate-stabilized AuNPs as a sensing probe. Not only a new absorption band appeared in the long wavelength field, but also an obvious and rapid color change from burgundy for individual AuNPs to purple for aggregated ones with the addition of VB1. The mechanism for the phenomena has been discussed with the aid of different characterization results and was attributed to the electrostatic interaction between AuNPs and VB1. The proposed method was rapid and highly sensitive, which could detect VB1 with the detection limit of 10.9 nM in the range of 30–650 nM within 15 min. Meanwhile, common ions and small biological molecules displayed negligible effect on the detection of VB1 indicating the high selectivity of the assay. Furthermore, the proposed colorimetric assay also has applied to the VB1 detection in tablets and human urine samples to prove its practicability.

Experimental

Materials and reagents

$HAuCl_4$, sodium citrate, H_3BO_3, $Na_2B_4O_7$, glucose, vitamin B3 (VB3) and folic acid (FA) were purchased from Shanghai Chemical Reagent Co., Ltd. (Shanghai, China). Vitamin B1 (VB1), ascorbic acid (Vc), tryptophan (Trp), dopamine (DA), uric acid (UA) were purchased from Aladdin Reagent Co., Ltd. (Shanghai, China). Vitamin B2 (VB2) was from Sinopharm Chemical Reagent Co., Ltd. (Shanghai, China). Vitamin B6 (VB6) was from Thermo Fisher Scientific Inc. (Fair Lawn, NJ, USA). All the other chemicals were of analytical grade except that VB2, VB3, FA and VB6 were biological reagents. Cation stock solutions used in this experiment were prepared from their chloride or nitrate salts. Cellulose membrane dialysis tubing (retained molecular weight: 1000 Da) was purchased from Sangon Biotech Co., Ltd (Shanghai, China). Ultrapure water (18.2 MΩ) from a Laboratory Ultrapure Water System (Kertone Water Treatment Co., Ltd, China) was used throughout the experiments.

Apparatus

Absorption spectra were obtained by a UV2600 spectrophotometer (Shimadzu, China) with a 1 cm quartz cell. Transmission electron microscopy (TEM) measurements were performed on a TECNAI F-20 electron microscope (JOEL 2100F, Netherlands) at an accelerating voltage of 200 kV. Fourier transform infrared (FTIR) spectra in the range of 400–4000 cm^{-1} were recorded on a Nicolet AVATAR 360 spectrophotometer. Zeta potential was detected using a Nano-ZS (Malvern Instruments, UK).

Synthesis of AuNPs

All the glassware was cleaned in a bath of freshly prepared *aqua regia* with volume ratio of HNO_3 : HCl to be 3 : 1, thoroughly rinsed with water, and dried in air. The AuNPs were prepared by employing sodium citrate as a stabilizer capped on the surface of AuNPs according to the previous reports.[29] Briefly, in a 250 mL round-bottomed flask equipped with a condenser, 100 mL 1 mM $HAuCl_4$ solution was added and heated to rolling boil with vigorous stirring. Then, 10 mL 38.8 mM sodium citrate was quickly added to the aboil solution and the mixture was kept boiling for another 30 min with sequential stirring. The color of mixed solution gradually changed from buff to colorless, then rapidly to grey and finally to burgundy, indicating the formation of AuNPs. Then the heating mantle was removed and let the solution cool to room temperature. At last, the AuNPs stock was obtained by filtering the solution through 0.22 μm membrane filter to remove the precipitate and stored in a refrigerator at 4 °C for future use.

Analytical procedure of VB1 detection

Typically, 200 μL H_3BO_3–$Na_2B_4O_7$ buffer solution (10 mM, pH 7.0) was mixed with 400 μL AuNPs, and then different amounts of VB1 were added into the mixture. The mixed solution was diluted to 2 mL with water. The absorption spectra of the mixed solution were implemented in the range of 400 nm to 890 nm after reacting for 15 min at room temperature. The absorbances at the wavelength of 523 nm and 710 nm were recorded. The absorbance variation $\Delta A_{710\ nm}/A_{523\ nm}$ $(= (A_{710\ nm}/A_{523\ nm})_{with\ VB1} - (A_{710\ nm}/A_{523\ nm})_{without\ VB1})$ was calculated. Meanwhile, the color changes were also recorded with photos. All experiments were performed in triplicate at room temperature.

Real sample analysis

According to the previous work,[17] seven pharmaceutical VB1 tablets produced by Huazhong Pharmaceutical Co., Ltd. had been grinded into powder. Then 0.3898 g powder was dissolved with 10 mL water and sonicated for 20 min. Then the solution was centrifuged at a speed of 4000 rpm for 10 min to remove the precipitate. Finally, 2 mL supernatant was filtered with 0.22 μm membrane filter, collected and diluted to 100 mL as the stock solution.

Human urine samples were obtained from healthy adult volunteers at Fujian Agriculture and Forestry University Hospital (informed consent was obtained from all human subjects). According to the previous report,[30] the urine samples were centrifuged at 8000 rpm for 10 min to eliminate the insoluble substance or any protein interference. Then, the supernatant was filtered with 0.22 μm membrane filter, and the filter were diluted 100-fold with ultrapure water for further analysis. All the spiked samples were prepared by adding different amounts of VB1 solutions to the diluted samples and analyzed according the experimental procedure described in section "Analytical procedure of VB1 detection".

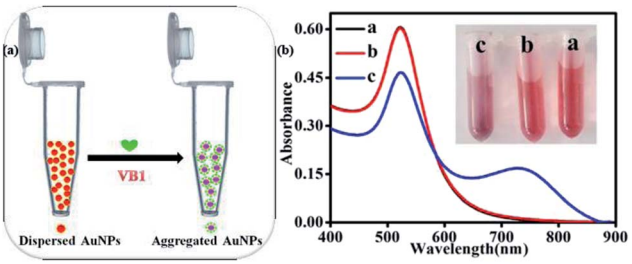

Fig. 1 (a) Schematic illustration for colorimetric detection of VB1 with AuNPs; (b) UV-Vis absorption spectra of AuNPs-VB1 system (inset: relative color photos for each curve. The contents for each curve were as follows: (a) AuNPs, (b) AuNPs + H_3BO_3 – $Na_2B_4O_7$, (c) AuNPs + H_3BO_3 – $Na_2B_4O_7$ + VB1. The usage for each substance: 400 μL AuNPs, 200 μL 10 mM pH = 7 H_3BO_3–$Na_2B_4O_7$ buffer solution and 60 μL 10 μM VB1).

Results and discussion

UV-Vis absorption spectra of AuNPs-VB1 system

As illustrated in Fig. 1a and inserted photo in Fig. 1b, the color of dispersed AuNPs changed from burgundy to purple as VB1 was added into AuNPs. According to the previous report, the color of AuNPs solution changing from burgundy to purple or blue even to gray is due to the aggregation of AuNPs induced by the analytes.[23] To investigate the reason for the phenomena, the UV-Vis spectra for the AuNPs in the absence and in the presence of VB1 have been scanned. As shown in Fig. 1b, the obtained AuNPs exhibited a strong LSPR band in the range of 450–850 nm with a characteristic peak at 523 nm in H_3BO_3–$Na_2B_4O_7$ buffer solution (Fig. 1b, curve b). When 300 nM VB1 was added, the intensity of the absorption peak at 523 nm gradually decreased and a new absorption band in the range of 600–890 nm appeared with the intensity enhancing (Fig. 1b, curve c). In this work, it was thought that the above observations were attributed to the aggregation of AuNPs induced by the electrostatic interactions between negatively charged AuNPs due to the citrate capping on their surface and positively charged VB1 molecules under the experimental conditions.[13,17]

Mechanism studies for the colorimetric detection of VB1 with AuNPs

In order to confirm the proposed assay mechanism, many characterizations have been carried out. Firstly, the size and morphologies of AuNPs in the absence and in the presence of VB1 had been explored with TEM. The TEM images displayed that AuNPs without the addition of VB1 were well dispersed (Fig. 2a) and roughly spherical in the range of 11–16 nm (inset in Fig. 2a) with an average size of 13.5 nm, while the obvious aggregation of AuNPs formed upon the addition of 300 nM VB1 (Fig. 2b). Moreover, the zeta potential of AuNPs was −46.7 eV indicating that AuNPs bear a negative charge due to the capping of citrate on their surface (Fig. S1a†). While the zeta potential decreased to −14.1 eV upon the addition of 300 nM VB1 into AuNPs (Fig. S1b†).

Furthermore, the FTIR spectra showed that the characteristic peaks for C=N$^+$ (1665 cm^{-1}), C=N (pyrimidine ring)

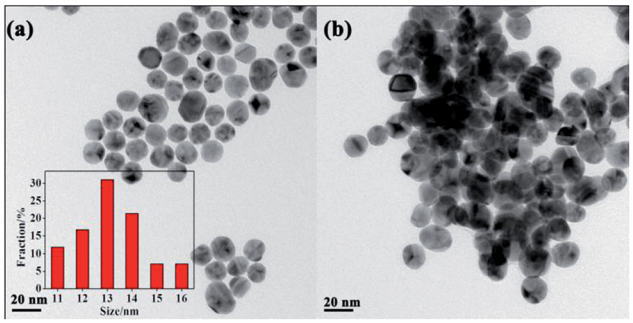

Fig. 2 TEM images of AuNPs (a) in the absence and (b) in the presence of 300 nM VB1.

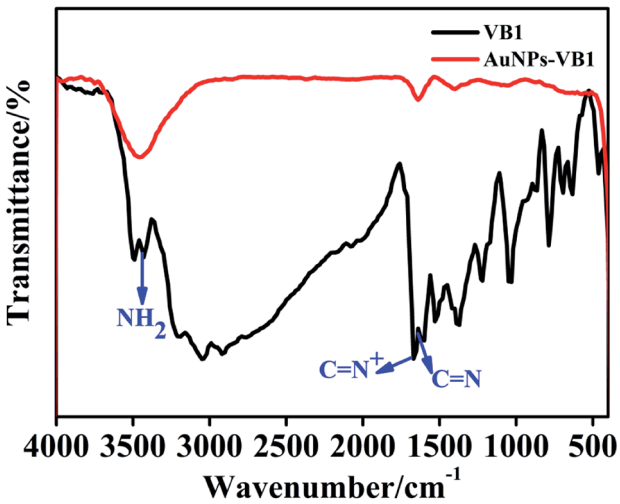

Fig. 3 FT-IR spectra of pristine VB1 and AuNPs-VB1 system.

(1618 cm^{-1}) and NH_2 stretching frequencies (3438 cm^{-1}) for VB1 changed with notable decreasing intensity in the AuNPs-VB1 system (Fig. 3), which was similar to the previous report that the aggregation of glutathione modified silver nanoparticles come out with the introduction of VB1.[13] Taking the above results into consideration, it came to the conclusion that the colorimetric detection of VB1 depended on the prevalence of electrostatic interaction between AuNPs and VB1.

Optimization of experimental conditions

Effect of pH value. It has reported previously that the LSPR of AuNPs was close to the dielectric constant of their surrounding medium,[23] the detection of VB1 was carried out in different pH values by adjusting with H_3BO_3–$Na_4B_2O_7$ buffer solution. Seen from Fig. 4, the pH played great effect on the detection of VB1 with AuNPs. When pH was lower than 7.0, the $\Delta A_{710\ nm}/A_{523\ nm}$ gradually increased with the enhancement of pH, while $\Delta A_{710\ nm}/A_{523\ nm}$ gradually decreased as pH increased from 7.0 to 11.0. Since colorimetric detection of VB1 with AuNPs was realized mainly based on the electrostatic interaction between AuNPs and VB1, the $\Delta A_{710\ nm}/A_{523\ nm}$ closely related to the charge of AuNPs and VB1. On the one hand, the protonation of citrate reduced the negative charge on the surface of AuNPs when the

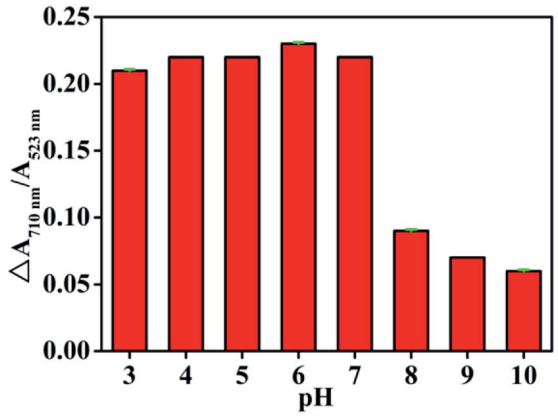

Fig. 4 Effect of pH on the colorimetric detection of VB1 with AuNPs.

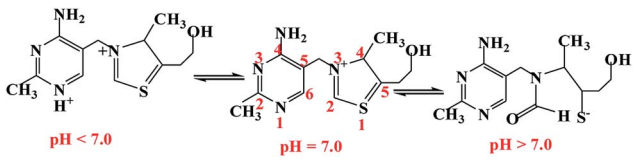

Fig. 5 pH-dependent forms of VB1 from cationic forms to the pseudobase and thiol forms.[14,31]

pH was too low. On the other hand, the structure and charge of VB1 varies with the pH values.[14,31] As depicted in Fig. 5, VB1 is positively charged on both the pyrimidine N1 nitrogen ($pK_{a1} \approx 4.8$) and thiazole N3 nitrogen at low pH, and the VB1 presents with a cation that a positive charge appears on the thiazole N3 nitrogen at physiological pH. Finally, the VB1 passes through an uncharged pseudobase intermediate to display in negatively charged thiol form ($pK_{a2} \approx 9.2$) with the pH further increasing. As a result, the same charge of AuNPs and VB1 repelled each other as pH was higher than 7. Therefore, pH = 7.0 was chosen as the experimental acidity in the following study.

Stability of the detection system. To investigate the stability of AuNPs for the detection of VB1, the response kinetics of AuNPs towards to VB1 were investigated for different times. As shown in Fig. S2,† the absorbance of AuNPs was quickly reduced within 15 min upon the addition of VB1 and remained constant when the reaction time prolonged to 30 min. These results indicated that the response rate was fast and that the absorbance could remained stable for a long time, promising the feasibility for rapid and stable detection of VB1.

Interference and selectivity. To evaluate the selectivity of the colorimetric response of AuNPs toward to VB1, the interferences from metal ions (Ag^+, Hg^{2+}, Cu^{2+}, Co^{2+}, Ni^{2+}, Pb^{2+}, Cd^{2+}, Fe^{2+} and Fe^{3+}), the relative vitamin B complexes (VB2, VB3, FA, Vc and VB6) and common biological small molecules (Trp, DA, UA and glucose) were studied. It was delighted to find that there was negligible absorbance change in the metal ions (Fig. 6a and c) and interfering molecules (Fig. 6b and d), indicating the excellent selectivity of the proposed assay.

Analytical performances of the VB1 detection. To explore the sensitivity of the VB1 detection, the $A_{710\ nm}/A_{523\ nm}$ evolution of AuNPs in the absence of different concentrations of VB1 was

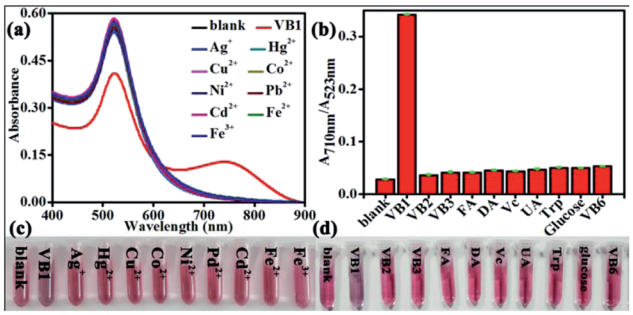

Fig. 6 Response of AuNPs to different (a) metal ions and (b) biological molecules; photographic images of color changes observed from AuNPs in different (c) metal ions and (d) biological molecules.

investigated. As shown in Fig. 7, the $A_{710\ nm}/A_{523\ nm}$ gradually increased up the addition of VB1 ranging from 30 nM to 2000 nM with the obvious color change observed by naked eyes. Meanwhile, the $\Delta A_{710\ nm}/A_{523\ nm}$ was in a distinct linear relationship with the VB1 concentration in the range 30–650 nM with a linear regression equation of $\Delta A_{710\ nm}/A_{523\ nm} = 0.0011C_{VB1} - 0.039$, a correlation coefficient (R) of 0.9912 and a detection limit of 10.9 nM. And obvious color change could be observed with naked eyes when 75 nM VB1 was added into AuNPs solution. It was pleased to find that the detection limit was comparable with or superior to those obtained from other sensitive methods (Table S1†). Moreover, the proposed assay was rapid, simple and could be observed with naked eyes.

Detecting VB1 in pharmaceutical tablets and urine samples. To demonstrate the practicability of the proposed method for the detection of VB1 in real samples, the proposed method has been applied to detection VB in pharmaceutical VB1 tablets and human urine samples. As presented in Table 1, the recoveries

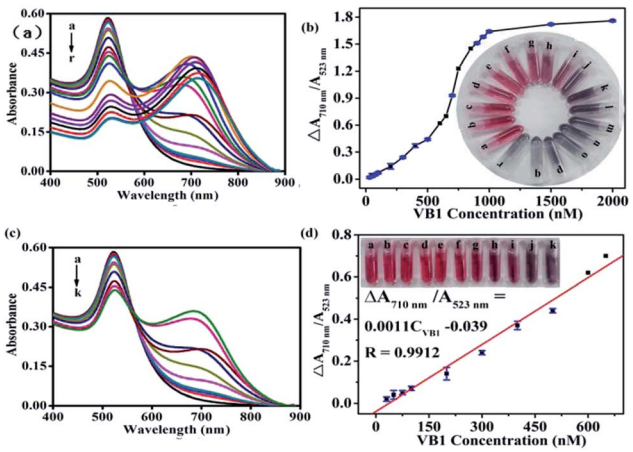

Fig. 7 (a) UV-Vis spectra of AuNPs and (b) relationship of $\Delta A_{710\ nm}/A_{523\ nm}$ with different concentrations of VB1 under optimum experimental conditions (inset: relative photographs of AuNPs in the presence of VB1 with the concentration from a to r to be 0, 30, 50, 75, 100, 200, 300, 400, 500, 600, 650, 700, 750, 800, 950, 1000, 1500 and 2000 nM, respectively); (c) UV-Vis spectra of AuNPs and (d) linear relationship of $\Delta A_{710\ nm}/A_{523\ nm}$ with the concentrations of VB1 in the range of 30–650 nM (inset: relative photographs of AuNPs in the presence of VB1 with the concentration from a to k to be 0, 30, 50, 75, 100, 200, 300, 400, 500, 600, 650 nM, respectively).

Table 1 Analytical results of VB1 in real samples ($n = 3$)

Samples	Detected/nM	Spiked/nM	Found/nM	Recovery/%	RSD/%
VB1 tablets	402.5	50	450.1	95.2	0.2
	402.5	100	451.2	97.4	0.3
Human urine samples	0	200	198.6	99.3	0.3
	0	400	401.3	100.3	0.4

were in the range of 95.2–97.4% for VB1 tablets and 99.3–100.3% for urine samples, indicating the applicability of this colorimetric assay for VB1 detection in real samples.

Conclusions

In this work, a rapid, simple, sensitive and selective colorimetric assay has been proposed for the detection of VB1 based on the aggregation of the AuNPs through electrostatic interaction between AuNPs and VB1. The assay was without any addition of any other metal salts or complex instrumentation. The proposed assay has been successfully applied to the quantitative detection of VB1 in urine samples and tablets, promising the potential application for monitoring VB1 related to biological filed.

Conflicts of interest

There are no conflicts to declare.

Acknowledgements

This research work was financially supported by the Nature Science Foundation from Science and Technology Department of Fujian Province (No. 2018J05013) and Education Research Project for Young and Middle-Aged Teachers of Fujian Province (JT180136), which were gratefully acknowledged.

References

1 A. B. Tayade, P. Dhar, J. Kumar, M. Sharma, O. P. Chaurasia and R. B. Srivastava, *Anal. Chim. Acta*, 2013, **789**, 65–73.
2 S. Shankar and S. A. John, *RSC Adv.*, 2015, **5**, 49920–49925.
3 S. Manzetti, J. Zhang and D. van der Spoel, *Biochemistry*, 2014, **53**, 821–835.
4 R. K. Gupta, S. K. Yadav, V. A. Saraswat, M. Rangan, A. Srivastava, A. Yadav, R. Trivedi, S. K. Yachha and R. K. Rathore, *Clin. Nutr.*, 2012, **31**, 422–428.
5 G. E. Gibson and J. P. Blass, *Antioxid. Redox Signaling*, 2007, **9**, 1605–1619.
6 K. C. Whitfield, G. Smith, C. Chamnan, C. D. Karakochuk, P. Sophonneary, K. Kuong, M. A. Dijkhuizen, R. Hong, J. Berger, T. J. Green and F. T. Wieringa, *PLoS Neglected Trop. Dis.*, 2017, **11**, e0005814.
7 E. Day, P. W. Bentham, R. Callaghan, T. Kuruvilla and S. George, *Cochrane Database Syst. Rev.*, 2013, **7**, CD004033.
8 G. E. Gibson, J. A. Hirsch, R. T. Cirio, B. D. Jordan, P. Fonzetti and J. Elder, *Mol. Cell. Neurosci.*, 2013, **55**, 17–25.
9 G. Zhang, H. Ding, H. Chen, X. Ye, H. Li, X. Lin and Z. Ke, *J. Nutr.*, 2013, **143**, 53–58.
10 K. Taguchi, E. Fukusaki and T. Bamba, *J. Chromatogr. A*, 2014, **1362**, 270–277.
11 M. Kamruzzaman, A. M. Alam, S. H. Lee and T. D. Dang, *Sens. Actuators, B*, 2013, **185**, 301–308.
12 J. Zhu, S. Liu, Z. Liu, Y. Li, M. Qiao and X. Hu, *RSC Adv.*, 2014, **4**, 5990–5994.
13 R. Rajamanikandan and M. Ilanchelian, *Sens. Actuators, B*, 2017, **244**, 380–386.
14 G. Perez-Caballero, J. F. Perez-Arevalo, E. A. Morales-Hipolito, M. E. Carbajal-Arenas and A. Rojas-Hernandez, *J. Mex. Chem. Soc.*, 2011, **55**, 126–131.
15 A. Bayandori Moghaddam, F. Gudarzy and Y. Ganjkhanlou, *J. Fluoresc.*, 2014, **24**, 1025–1030.
16 Y. Li, P. Wang, X. Wang, M. Cao, Y. Xia, C. Cao, M. Liu and C. Zhu, *Microchim. Acta*, 2010, **169**, 65–71.
17 Y. Luo, H. Miao and X. Yang, *Talanta*, 2015, **144**, 488–495.
18 S. Shankar and S. A. John, *RSC Adv.*, 2015, **5**, 49920–49925.
19 R. Purbia and S. Paria, *Biosens. Bioelectron.*, 2016, **79**, 467–475.
20 F. Nemati, R. Zare-Dorabei, M. Hosseini and M. R. Ganjali, *Sens. Actuators, B*, 2017, **255**, 2078–2085.
21 S. Liu, Y. Chen, Z. Liu, X. Hu and F. Wang, *Microchim. Acta*, 2006, **154**, 87–93.
22 K. W. Huang, C. J. Yu and W. L. Tseng, *Biosens. Bioelectron.*, 2010, **25**, 984–989.
23 D. Vilela, M. C. Gonzalez and A. Escarpa, *Anal. Chim. Acta*, 2012, **751**, 24–43.
24 N. Y. Chen, H. Y. Liu, Y. J. Zhang, Z. W. Zhou, W. P. Fan, G. C. Yu, Z. Y. She and A. G. Wu, *Sens. Actuators, B*, 2018, **255**, 3093–3101.
25 Y. M. Leng, Y. L. Li, A. Gong, Z. Y. Shen, L. Chen and A. G. Wu, *Langmuir*, 2013, **29**, 7591–7599.
26 Y. L. Li, Y. M. Leng, Y. J. Zhang, T. H. Li, Z. Y. Shen and A. G. Wu, *Sens. Actuators, B*, 2014, **200**, 140–146.
27 T. H. Li, Y. L Lia, Y. J. Zhang, C. Dong, Z. Y. Shen and A. g. Wu, *Analyst*, 2015, **140**, 1076–1081.
28 G. H. Wu, C. Dong, Y. L. Li, Z. Q. Wang, Y. X. Gao, Z. Y. Shen and A. G. Wu, *RSC Adv.*, 2015, **5**, 20595–20602.
29 K. C. Grabar, R. G. Freeman, M. B. Hommer and M. J. Natan, *Anal. Chem.*, 1995, **67**, 735–743.
30 P. K. Brahman, R. A. Dar and K. S. Pitre, *Sens. Actuators, B*, 2013, **117**, 807–812.
31 K. A. Edwards, N. Tu-Maung, K. Cheng, B. Wang, A. J. Baeumner and C. E. Kraft, *ChemistryOpen*, 2017, **6**, 178–191.